

# Application of Density Functional Theory To Study the Double Layer of an Electrolyte with an Explicit Dimer Model for the Solvent

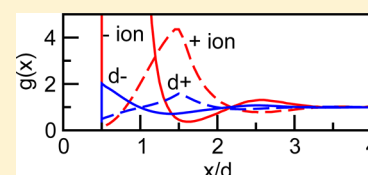
Douglas Henderson,<sup>\*,†</sup> De-en Jiang,<sup>‡</sup> Zhehui Jin,<sup>§</sup> and Jianzhong Wu<sup>\*,§</sup>

<sup>†</sup>Department of Chemistry and Biochemistry, Brigham Young University, Provo, Utah 84602-5700, United States

<sup>‡</sup>Chemical Sciences Division, Oak Ridge National Laboratory, Oak Ridge, Tennessee 37831, United States

<sup>§</sup>Department of Chemical and Environmental Engineering, University of California, Riverside, California 92521-0425, United States

**ABSTRACT:** Most theoretical studies of an electrical double layer, which is formed by an electrolyte in contact with a charged electrode, employ a primitive model in which the solvent is represented by a dielectric continuum. This implicit-solvent model is convenient because computations are comparatively simple. However, it suppresses oscillations in the density profiles of ionic species that result from the discreteness of the solvent molecules. Furthermore, the implicit-solvent model yields poor results for the capacitance. In comparison with experiment at fixed electrode charge density, it predicts a too small electrode potential, and the resultant capacitance is too large. This latter discrepancy can be compensated in part by postulating the existence of an often fictitious inner layer whose properties are parametrized to agree best with experiment. The use of an implicit solvent model and an inner layer helps in correlating experimental results but rests on a faulty microscopic picture. Unfortunately, explicit consideration of solvent molecules poses both theoretical and numerical difficulties and, as a result, studies using an explicit solvent model have been few and far between. In this study, we consider a simple nonprimitive or explicit solvent model in which each solvent molecule is represented by a dimer composed of touching positive and negative hard spheres, with a resulting dipole moment that is equal to that of a water molecule, and the ions are represented by charged hard spheres. The density profiles and charge–potential relationship of this model are examined using the classical density functional theory. We find that the introduction of an explicit solvent increases the electrode potential, at fixed electrode charge, without the need to postulate a parametrized inner layer. Because of the solvent polarity, the ion profiles become strong oscillatory and show local charge inversion near a highly charged electrode surface at all ion concentrations.



## 1. INTRODUCTION

Almost all theoretical studies of an electric double layer (EDL), which is formed by ions in contact with a charged surface, employ the primitive model (PM) in which the ions are represented by charged hard spheres and the solvent by a dielectric continuum. In this model, the electrostatic interaction is inversely scaled with a dielectric constant that equals that of the bulk solvent. If all hard spheres have the same diameter designated as  $d$ , the PM is called the restricted primitive model (RPM). The popular Gouy–Chapman–Stern (GCS) theory<sup>1–3</sup> makes a further approximation that the size of the ionic spheres may be neglected. The GCS theory predicts that the ionic densities, local charge, and potential profiles are all monotonic. Most molecular simulations<sup>4–6</sup> and modern theories of electrochemistry<sup>7–15</sup> retain the GCS or PM framework but include a nonzero ion diameter ( $d$  in the RPM). Because of the ion size and electrical correlations, simulations and modern theories show EDL properties different from those predicted by the GCS theory. In particular, the profiles need not be monotonic, especially in the presence of multivalent ions. However, simulation and modern theories based on the PM give the potential of the electrode, for a given electrode charge density, that is too small compared to experimental results. A conventional way of dealing with this problem is to assume that the dielectric properties of the region near the electrode (often called the inner layer or Stern layer)

differ from those of the region further away from the electrode (often called the diffuse layer). For example, the dielectric constant in the inner layer (IL) is assumed to be smaller than that in the diffuse layer (DL). This results in a larger potential difference across the IL (called the inner layer potential). Another possible modification, also resulting in an increased IL potential, is to assume that the thickness of the IL is greater than the distance of closest approach suggested by the PM. The rationale for such modifications is the presence of a presumed layer of adsorbed, and not freely oriented, solvent molecules, that excludes the ions. The properties of the postulated IL are presumed to be independent of the ion concentrations and can be adjusted to fit the experiment. A recent review<sup>16</sup> summarizes this approach. The problem with such an approach is that it is semiempirical and presumes that the ionic density profiles are the same (just shifted) as those of the PM.

A more satisfying approach is to use a nonprimitive model, i.e., a model with explicit consideration of the solvent molecules. The simplest nonprimitive model uses hard spheres to represent the solvent molecular volume and a dielectric background to represent the energetic effects. This has been called the solvent primitive model (SPM) or molecular solvent

Received: June 1, 2012

Revised: July 20, 2012

Published: August 13, 2012

model (MSM).<sup>17–19</sup> The SPM is certainly an improvement over the PM. The density profiles are oscillatory. However, the electrostatic properties are not much improved and an IL with a reduced dielectric constant is still needed to yield a larger electrode potential. The ion–dipole model is more realistic; here the ions are represented by hard spheres, and the solvent molecules are represented by hard spheres each with an embedded point dipole at the center. The advantage of the ion–dipole model is that an analytic solution for the electrode potential can be obtained<sup>20,21</sup> using an integral equation theory called the mean spherical approximation (MSA). Because the MSA is a linear response theory, the results are applicable only for systems with small electrode charge. Moreover, the MSA does not yield useful expressions for the ionic density and potential profiles. Nevertheless, it does predict that the interfacial inhomogeneity for the solvent molecules is not restricted to a narrow region near the electrode but extends over the entire EDL. In the MSA, a separation of the potential into a term similar to that of a DL and an IL-like term that is independent of the electrolyte concentration is valid at least at low concentrations; it breaks down only when the electrolyte concentration is sufficiently high. There have been integral equation studies using somewhat more realistic solvent models<sup>22,23</sup> but they have not been as intensively studied as the MSA. Some simulations that employ a fairly realistic model for water<sup>24,25</sup> have been made. The difficulty with such simulations is that they are possible only at fairly high electrolyte concentrations. Even at a concentration of 1 M, there are about 55 water molecules for each ion. At 0.01 M, there would be about 5500 water molecules for each ion. Enormous computational time would be required to obtain good statistics for the ionic properties. As a result, calculations have been made only for relatively high ionic concentrations ( $\sim 1$  M). No doubt it will be possible to consider low concentrations in the future but this seems out of the question at present. The integral equations, such as those of Woelki,<sup>26,27</sup> may be useful for such models. The agreement of the results of these integral equations is fairly good. An application of this method has been made for the RPM.<sup>28</sup> Using the hypernetted chain closure, the agreement with simulations is reasonable as long as the electrode charge is not too great.

In this work, we are interested to identify microscopic origins underlying the differences between implicit and explicit models for the solvent. To examine the EDL behavior, we use a version of density functional theory (DFT) that was developed for dimers and ions.<sup>29</sup> The solvent molecules are modeled as neutral dimers, consisting of touching positively and negatively charged hard spheres with a dipole moment equal to that of a water molecule. The ions are modeled as charged positive and negative hard spheres. While a dimer is a fairly crude model of water, it is a good start to include explicit solvent effects and should yield useful, possibly qualitative, insights. Moreover, we are able to get beyond the linear regime and, as a result, this work is a step beyond the MSA. Recently, this extended dipole model for an electrolyte solvent has been applied, with pleasing success, to study the capacitance of an organic electrolyte in slit pores.<sup>30</sup> The DFT approach for a dimer has been checked by simulation<sup>31</sup> in an application for an ionic liquid and has been found to be quite accurate, especially for the response of the electrolyte to the charge of the electrode.

## 2. MOLECULAR MODEL AND THEORY

Our nonprimitive model consists of hard sphere ions and a hard-sphere dimer solvent with the dipole moment the same as that of a water molecule in the vacuum. In other words, each solvent molecule is represented by a pair of positive and negative spheres that are tethered to form a dimer of touching spheres. The interaction potential between any pair of hard spheres,  $i$  and  $j$ , whose centers are separated by distance  $r$ , is given by

$$\beta u_{ij}(r) = \begin{cases} \infty, & r < d \\ Z_i Z_j l_B / r, & r > d \end{cases} \quad (1)$$

where  $\beta = 1/(k_B T)$  with  $k_B$  and  $T$  being the Boltzmann constant and the absolute temperature, respectively. Parameter  $d$  is the diameter of the hard spheres, which is taken to be equal for all species. Here we use  $d = 2$  Å, to give a reasonable size for the pseudo-water solvent molecules. A common diameter,  $d = 2$  Å, is chosen only for simplicity. In our DFT, the ions and dimer constituents can all have different diameters and such possibilities can be the subject for future studies. Of course, the shape of a water molecule is closer to a sphere than a dimer and it has tetrahedral symmetry. However, the dimer solvent represents a reasonable first approximation and is one for which we can obtain analytical results. This value of  $d$  is also fairly reasonable for  $\text{Li}^+$  and  $\text{F}^-$  ions. The valences,  $Z_i$ , are  $\pm 0.1926$  for the two spheres in the dimer, and  $\pm 1$  for the ions. The values chosen for the dimer valences and diameters correspond to the dipole moment of water, 1.85 D. We note that the MSA yields a dielectric constant for a given dipole moment that is too small. DFT does not yield an expression or a numerical value for the dielectric constant that results from a given dipole moment. However, the MSA is a linear response theory and a small dielectric constant is not too surprising. DFT is a nonlinear theory and should not share this problem. The parameter  $l_B = \beta e^2 / 4\pi \epsilon_0 \epsilon_r$  is the Bjerrum length, where  $e$  is the magnitude of the elementary charge,  $\epsilon_0$  is the permittivity of free space, and  $\epsilon_r$  is the background or residual relative permittivity or dielectric constant of the system. The smallest value that we could use, and still have the DFT equations yield a convergent result, was  $\epsilon_r = 4$ . This is a bit larger than we desired but still yields informative results. The charges of the spheres are assumed to be located at their centers. In our previous DFT work for the RPM for an aqueous system, we used the value  $l_B = 7.14$  Å, which corresponds to an aqueous electrolyte at room temperature. Here we used  $l_B = 139.23$  Å, which corresponds to a system with a molecular solvent with a residual dielectric constant  $\epsilon_r = 4$ .

The interaction of a charged sphere with the electrode is given by

$$\beta W_i(x) = \begin{cases} \infty, & x < d/2 \\ -2\pi l_B Z_i \sigma x / e, & x > d/2 \end{cases} \quad (2)$$

where  $x$  is the perpendicular distance of the center of the sphere from the electrode surface. Parameter  $\sigma$  stands for the surface charge density of the electrode, which is assumed to be planar, smooth, and nonpolarizable. The electrode charge is located on the surface, that is, zero skin depth. Because we have focused on the relation between the electric potential and the surface charge in the presence of an electrolyte solution, the properties of the electrode are secondary.

The structure of the interface is described by the density profiles of the ions,  $\rho_i(x)$ , which give the local number densities of the ions of species  $i$  as a function of the perpendicular distance  $x$  from the electrode surface. According to the density functional theory (DFT), the normalized density profiles for spherical ions,  $g_i(x) = \rho_i(x)/\rho_i(\infty)$ , are calculated from

$$g_i(x) = \exp\{-\beta Z_i e \psi(x) - \beta \Delta \mu_i^{\text{ex}}(x)\} \quad (3)$$

where  $\Delta \mu_i^{\text{ex}}(x)$  stands for the deviation of the local excess chemical potential from that of the bulk solution and is given by

$$\mu_i^{\text{ex}} = \delta[F_{\text{hs}}^{\text{ex}} + F_{\text{chain}}^{\text{ex}} + F_{\text{ec}}^{\text{ex}}]/\delta \rho_i(z) \quad (4)$$

In eq 4,  $\mu_i^{\text{ex}}$  stands for the excess chemical potential of particle  $i$  in a reference bulk fluid with ionic densities  $\{\rho_i(\infty)\}$ ;  $F_{\text{hs}}^{\text{ex}}$ ,  $F_{\text{chain}}^{\text{ex}}$ , and  $F_{\text{ec}}^{\text{ex}}$  account for, respectively, the intrinsic Helmholtz energy due to the ionic size, the dimer chain connectivity, and the electrostatic correlations. As detailed in a previous work,<sup>29</sup>  $F_{\text{hs}}^{\text{ex}}$  is represented by a modified fundamental measure theory,  $F_{\text{chain}}^{\text{ex}}$  is from an extension of the thermodynamic perturbation theory for inhomogeneous systems, and  $F_{\text{ec}}^{\text{ex}}$  is formulated in terms of a quadratic density expansion of the excess Helmholtz energy with respect to that of a uniform ionic system with the input of the direct correlation functions obtained from the MSA.

The quantity,  $\psi(x)$ , is related to the local electric potential. The latter is calculated by an integration of the Poisson equation:

$$\psi(x) = \frac{e}{\epsilon_0 \epsilon_r} \sum_i Z_i \int_x^\infty dx' (x - x') \rho_i(x') \quad (5)$$

In our DFT algorithm, it is convenient to write eq 5 in the form

$$\begin{aligned} \psi^*(x) &\equiv \beta e \psi(x) \\ &= \psi^*(0) + 4\pi l_B \sum_i \left[ \int_x^\infty dx' x Z_i \rho_i(x') \right. \\ &\quad \left. + \int_0^x dx' x' Z_i \rho_i(x') \right] \end{aligned} \quad (6)$$

Intuitively, eq 3–6 can be understood as a generalization of the Poisson–Boltzmann (PB) equation for ionic distributions. Unlike the conventional PB equation for charged systems, however, the DFT accounts for the ionic excluded volume and electrostatic correlation effects. While both effects are ignored in the GCS theory, we expect that they play an important role in the nonprimitive model because it entails direct electrostatic interactions.

Because the ionic local excess chemical potentials are related to the ion–solvent interactions, their density profiles near an electrode must be solved together with the distribution of the solvent molecules. In this work, the normalized density profiles for the solvent segments are calculated from

$$\begin{aligned} g_+(x) &= \exp\{\lambda_+(x)\} \int dx' \exp\{\lambda_-(x')\} \\ &\quad \times \theta(d - |x - x'|)/2d \end{aligned} \quad (7)$$

$$\begin{aligned} g_-(x) &= \exp\{\lambda_-(x)\} \int dx' \exp\{\lambda_+(x')\} \\ &\quad \times \theta(d - |x - x'|)/2d \end{aligned} \quad (8)$$

where  $\lambda_\pm(x) = -\beta Z_\pm e \psi(x) - \beta \Delta \mu_\pm^{\text{ex}}(x)$  stands for the local potential of a solvent segment.

Similar to most integral equation approaches, eqs 4–8 are solved numerically with an iteration procedure (Picard iteration in our case). Once the ionic density profiles are determined, the charge density of the interface is determined from

$$\sigma = -e \sum_i Z_i \int_{d/2}^\infty dx' \rho_i(x') \quad (9)$$

Because of electrostatic neutrality, the charge density of the interface must be equal in magnitude, but opposite in sign, to the integrated charge density of the mobile ions. Otherwise, there would be an electric field infinitely far from the electrode. The values of  $\rho_i(x)$  are such that  $\rho_i(\infty) = \rho_i = N_i/V$ , where  $N_i$  and  $V$  are the number of spheres of species  $i$  and the volume of the bulk system, respectively. Thus,  $\rho_i$  is simply the bulk number density of ions of species  $i$ .

We use dimensionless units throughout this work, namely,  $\sigma^* = \sigma d^2/e$ ,  $\psi^*(x) = \beta e \psi(x)$ , reduced ionic densities  $\rho_i^*(x) = \rho_i(x)d^3$ , and reduced temperature  $T^* = d/l_B$ . We consider ion concentrations of 0.01, 0.1, and 1 M. These concentrations correspond to the reduced densities for the anions and cations of  $4.82 \times 10^{-5}$ ,  $4.82 \times 10^{-4}$ , and  $4.82 \times 10^{-3}$ . The reduced segment density of the pseudo-water dimer model solvent is fixed at 0.268, which corresponds to 55.56 M for water. Results are presented for this explicit solvent model using the extended dipole with  $l_B = 139.23$  Å and, for comparison, we performed the DFT calculations for the RPM or implicit solvent model using  $l_B = 7.14$  Å and the same ionic densities but a vanishing dipole density. The implicit solvent model that we consider represents the same physical system as the explicit solvent model but with the additional approximation that the solvent molecules can be replaced by a continuum whose dielectric constant is that of water.

### 3. RESULTS

In Figure 1, the electrostatic potential of the electrode,  $\psi^*(0)$ , as a function of the electrode charge density is plotted using the

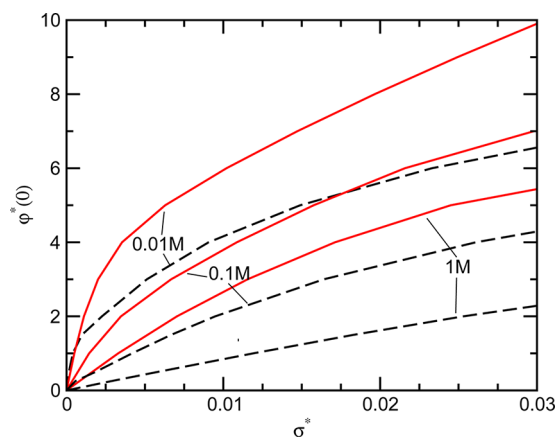


**Figure 1.** Dimensionless electrode potential,  $\psi^*(0)$ , as a function of the dimensionless electrode charge,  $\sigma^*$ , for the explicit (solid curve) and implicit (dashed curve) solvent models.

explicit and implicit solvent models for electrolyte concentrations of 0.01, 0.1, and 1 M. Unfortunately, we were able to obtain convergence of the DFT equations in the explicit solvent case only for comparatively small values of  $\psi^*(0)$ . We considered iteration methods other than the Picard scheme but did not have success. Although this was a disappointment,

our results do extend beyond the linear regime and do represent an advance over the MSA that is limited to the linear regime. We note that convergence problems for systems with high coupling constants is not an uncommon problem. For example, Federov et al.<sup>32</sup> made their simulations of an ionic liquid at a higher dimensionless temperature, which is equivalent to the use of a residual dielectric constant. We find that the potential is appreciably larger for the explicit solvent model than for the equivalent implicit solvent case. This is seen in Figure 1 and agrees with past experience with the MSA.<sup>33,34</sup> To obtain reasonable results for the potential (or capacitance) from the implicit solvent or RPM, it is conventional to postulate an IL with a reduced dielectric constant or extra width and a resultant increase in  $\psi^*(0)$ . For this enhanced IL picture to make sense, the difference between  $\psi^*(0)$  for the explicit and implicit solvent models should be independent of concentration (although not necessarily independent of electrode charge or potential). The difference,  $\Delta\psi^*(0)$ , between the explicit and implicit solvent model values of  $\psi^*(0)$  for the same electrode charge is plotted in Figure 2.

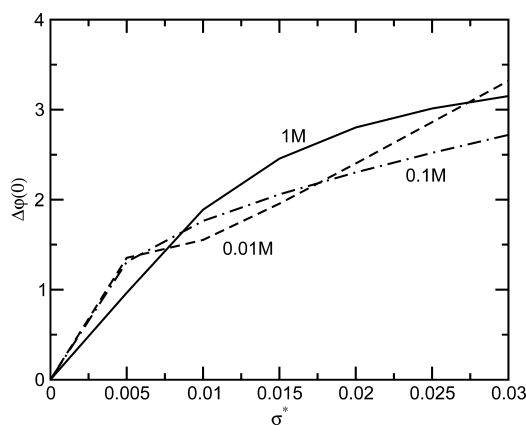


**Figure 2.** Difference,  $\Delta\psi^*(0)$ , between the dimensionless electrode potentials of the explicit and implicit solvent models, calculated using the same ion charge, diameter, temperature, and concentration, and for the same value of the dimensionless electrode charge.

Figure 2 is similar in spirit to a Parsons–Zobel plot.<sup>35</sup> However, we do not plot using the GCS capacitance as a variable, as was done by Parsons and Zobel, since our goal is not to test the applicability of the GCS theory but only to see if an IL correction to the RPM makes sense. The results of the MSA<sup>20,21</sup> and recent simulations<sup>36</sup> demonstrate that an inner layer correction is only valid as a first-order correction to  $\psi^*(0)$  that is useful only at low concentrations. The purpose of Figure 2 is to examine whether a parametrized IL can, in part, account for the low value of  $\psi^*(0)$  that results from the use of an implicit solvent model. As we have mentioned,  $\Delta\psi^*(0)$  should be calculated by taking the difference between  $\psi^*(0)$  as obtained from the explicit and implicit models for the same value of  $\sigma^*$ . It is not convenient to do this directly since DFT uses the potential as the input variable. Using a polynomial, we fit the DFT results for  $\psi^*(0)$  as a function of  $\sigma^*$  from the explicit and implicit solvent models for the three concentrations that we considered and used these polynomials to obtain  $\Delta\psi^*(0)$ . There is a small quantitative uncertainty due to the difficulty in obtaining a solution at small electrode charge and concentration. The curves are quantitatively correct. As is seen

in Figure 2,  $\Delta\psi^*(0)$  is, to a good approximation, independent of electrolyte concentration.

However, the results of Figure 2 do not imply that the inner-layer picture is valid on a microscopic level. The ion and dipole sphere profiles,  $g_i(x) = \rho_i(x)/\rho_i(\infty)$ , are plotted in Figure 3 for 0.01, 0.1, and 1 M. Oscillations in the ion and solvent sphere

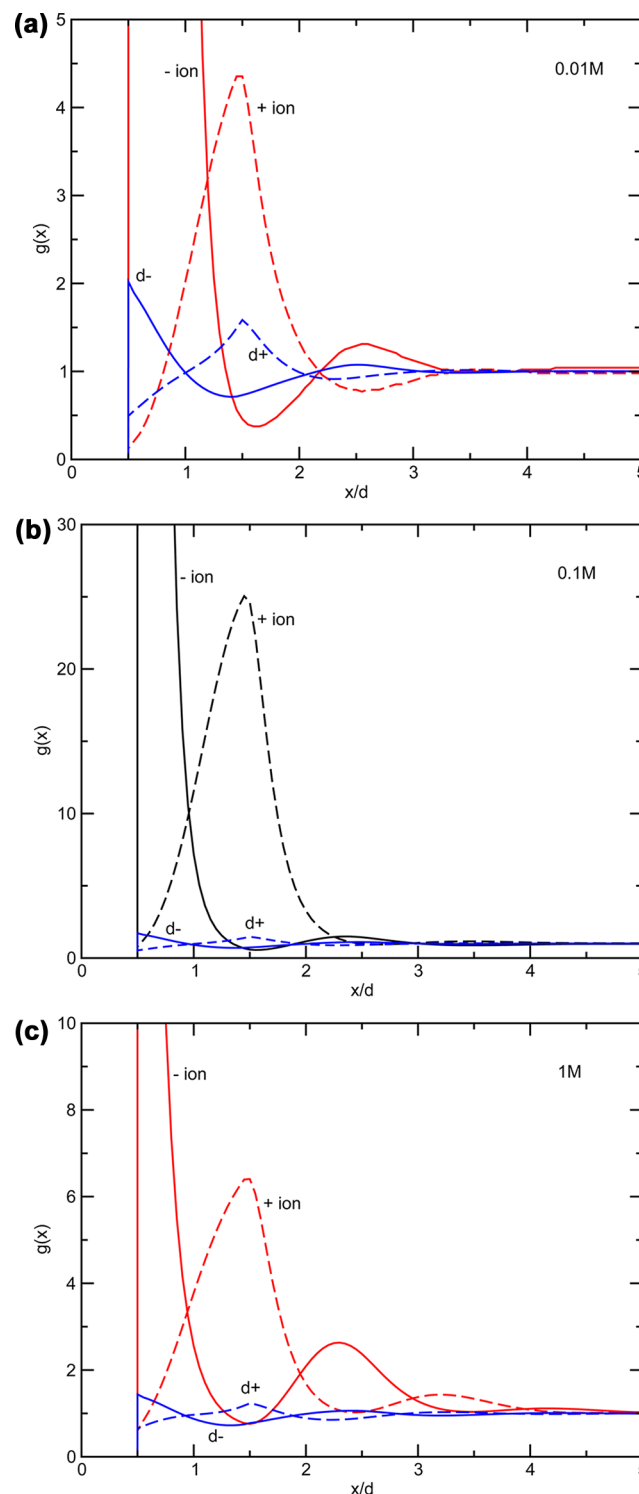


**Figure 3.** Dimensionless density profiles for the ion and dipole spheres using the explicit solvent model. Panel a is for 0.01 M with  $\psi^*(0) = 10$ , panel b is for 0.1 M with  $\psi^*(0) = 7$ , and panel c is of 1 M with  $\psi^*(0) = 5$ .



profiles are apparent for the explicit solvent model. In contrast to the implicit solvent model, charge inversion is present for a monovalent electrolyte at all concentrations. In the implicit solvent or RPM case, oscillations and charge inversion are present only at high concentrations and for electrolytes with multivalent ions. Because of chain connectivity between two spheres in the dimer solvent, Figure 3 shows a discontinuity in the slope of the dimer profiles at  $x = 1.5d$ . The structure of the solvent molecules is not confined to an inner layer. In agreement with the MSA results for the ion–dipole mixture,<sup>33,34</sup> the interfacial region of the solvent molecules is as broad as that of the ions. This is sensible as the solvent molecules orient under the influence of the electric field that is screened by the ions. As long as the charge profile has not vanished, there will be an electric field and an interfacial solvent region. For comparison, profiles are plotted for zero electrode charge and 1 M in Figure 4. The profiles of the two ends of the

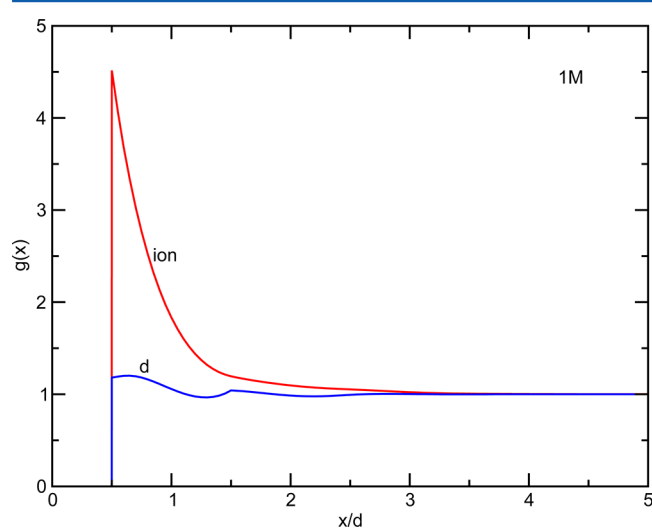


**Figure 4.** Dimensionless density profiles for the ion and dipole spheres near an uncharged electrode using the explicit solvent model for 1 M.

solvent molecule and the ions are independent of the charge of the spheres. The solvent profile is, apart from a discontinuity in slope, nearly independent of the distance from the electrode. Even though the electrode is uncharged, the ions are pushed against the electrode by the osmotic pressure of the ions.

#### 4. SUMMARY

Density functional theory has been applied to study the interfacial or double layer structure of an electrolyte using an explicit extended dipole model for the solvent. Although using a different model of the solvent, this study supplements and extends earlier studies that employed the MSA and a point dipole model for the solvent. We find that the use of an explicit solvent increases the electrode potential, at fixed electrode charge, without the need to postulate a parametrized inner layer. The ion profiles are oscillatory and show charge inversion near a highly charged surface at all ionic concentrations. In contrast to the MSA, this study is not limited to zero electrode charge. However, results for high electrode charge could not be obtained because of convergence problems. Perhaps the use of a larger ion diameter or more sophisticated convergence algorithms will help. This will be considered in future studies. In any case, we have obtained informative results outside the linear response regime. We hope to supplement this DFT study

with simulations, using methods already developed,<sup>31</sup> in the near future.

Unfortunately, the DFT equations would not yield a convergent result unless a residual background dielectric constant greater than unity was assumed. In this study, a residual background dielectric constant of 4 was used. Even then, the equations would converge only for relatively small electrode potentials. Nonetheless, our results provide useful insights. Without the use of a parametrized inner layer, the electrode potential is larger than the results obtained from the corresponding implicit model. Moreover, the interfacial region of the solvent molecules extends over the entire double layer and is not confined to an inner layer as is usually assumed.

In this work, we considered water since it is the most widely used solvent in electrochemistry. Jiang et al.<sup>30</sup> applied the dimer model to study the adsorption of an organic electrolyte in slit pores and did not encounter convergence problems. It is possible that solvents with lower dipole moments will pose fewer convergence problems. This will be investigated. In any case, our conclusions that an empirically parametrized inner layer is unnecessary to yield lower capacitance, or an increased electrode potential, than that predicted by an implicit solvent model and that, in contrast to conventional thought, the thickness of the solvent interfacial layer matches the thickness of the interfacial ion layer should be independent of the details of the explicit solvent model and the approximations of the DFT.

#### AUTHOR INFORMATION

##### Corresponding Author

\*E-mail: doug@chem.byu.edu (D.H.); jwu@engr.ucr.edu (J.W.).

##### Notes

The authors declare no competing financial interest.

#### ACKNOWLEDGMENTS

This work is in part supported by the Fluid Interface Reactions, Structures, and Transport (FIRST) Center, an Energy Frontier Research Center funded by the US Department of Energy, Office of Science, Office of Basic Energy Sciences (D.J.), the National Science Foundation (NSF-CBET-0852353), and the US Department of Energy (DE-FG02-06ER46296).

#### REFERENCES

- (1) Gouy, M. *J. Phys. (Paris)* **1910**, 9, 457–468.
- (2) Chapman, D. L. *Philos. Mag.* **1913**, 25, 475–481.
- (3) Stern, O. *Z. Elektrochem.* **1924**, 30, 508–561.
- (4) Torrie, G. M.; Valleau, J. P. *J. Chem. Phys.* **1980**, 73, 5807–5816.
- (5) Torrie, G. M.; Valleau, J. P. *J. Phys. Chem.* **1982**, 86, 3251–3257.
- (6) Boda, D.; Fawcett, W. R.; Henderson, D.; Sokolowski, S. *J. Chem. Phys.* **2002**, 116, 7170–7176.
- (7) Blum, L. *J. Phys. Chem.* **1977**, 81, 136–147.
- (8) Blum, L. *Theor. Chem.* **1980**, 5, 1–66.
- (9) Lozada-Cassou, M.; Saavedra-Barrera, R.; Henderson, D. *J. Chem. Phys.* **1982**, 77, 5150–5156.
- (10) Lozada-Cassou, M.; Henderson, D. *J. Phys. Chem.* **1983**, 87, 2956–2959.
- (11) Outhwaite, C. W.; Bhuiyan, L. B. *J. Chem. Soc., Faraday Trans. 2* **1983**, 79, 707–718.
- (12) Rosenfeld, Y. *J. Chem. Phys.* **1993**, 98, 8126–8148.
- (13) Yu, Y. X.; Wu, J. Z.; Gao, G. H. *J. Chem. Phys.* **2004**, 120, 7223–7233.
- (14) DiCaprio, D.; Stafiej, J.; Badiali, J.-P. *Mol. Phys.* **2003**, 101, 2545–2558.

- (15) DiCaprio, D.; Badiali, J.-P. *J. Phys. A* **2008**, *41*, 125401.
- (16) Henderson, D.; Boda, D. *Phys. Chem. Chem. Phys.* **2009**, *11*, 3822–3830.
- (17) Zhang, L.; Davis, H. T.; White, H. S. *J. Chem. Phys.* **1993**, *98*, 5793–5799.
- (18) Boda, D.; Chan, K.-Y.; Henderson, D. *J. Chem. Phys.* **1999**, *110*, 5346–5350.
- (19) Lamperski, L.; Zydor, A. *Electrochim. Acta* **2007**, *52*, 2429–2436.
- (20) Carnie, S. L.; Chan, D. Y. C. *J. Chem. Phys.* **1980**, *73*, 2949–2957.
- (21) Blum, L.; Henderson, D. *J. Chem. Phys.* **1981**, *74*, 1902–1910.
- (22) Torrie, G. M.; Patey, G. N. *J. Phys. Chem.* **1993**, *97*, 12909–12918.
- (23) Vossen, M.; Forstmann, F. *Mol. Phys.* **1995**, *86*, 1493–1516.
- (24) Spohr, E. *Electrochim. Acta* **2003**, *49*, 23–27.
- (25) Crozier, P.; Rowley, R. L.; Henderson, D. *J. Chem. Phys.* **2000**, *113*, 9202–9207.
- (26) Woelki, S.; Kohler, H.-H.; Krienke, H. *J. Phys. Chem. B* **2007**, *111*, 13386–13397.
- (27) Woelki, S.; Kohler, H.-H.; Krienke, H. *J. Phys. Chem. B* **2008**, *112*, 3365–3374.
- (28) Woelki, S.; Henderson, D. *Condens. Matter Phys.* **2011**, *14*, 43801.
- (29) Wu, J.; Jiang, T.; Jiang, D.; Zhehui, J.; Henderson, D. *Soft Matter* **2011**, *7*, 11222–11231.
- (30) Jiang, D.; Zhehui, J.; Henderson, D.; Wu, J. *Phys. Chem. Lett.* **2012**, *3*, 1727–1731.
- (31) Bhuiyan, L. B.; Lamperski, S.; Wu, J.; Henderson, D. *J. Phys. Chem. B* **2012**, *116*, 10364–10370.
- (32) Federov, M. V.; Georgi, N.; Kornyshev, A. A. *Electrochem. Commun.* **2010**, *12*, 296–299.
- (33) Carnie, S. L.; Chan, D. Y. C. *J. Chem. Phys.* **1980**, *73*, 2949–2957.
- (34) Blum, L.; Henderson, D. *J. Chem. Phys.* **1981**, *74*, 1902–1910.
- (35) Parsons, R.; Zobel, F. G. R. *J. Electroanal. Chem.* **1965**, *9*, 333–348.
- (36) Lamperski, S.; Henderson, D. *Mol. Sim.* **2011**, *37*, 264–268.